ISPRS Journal of Photogrammetry and Remote Sensing 66 (2011) 642–651

Contents lists available at ScienceDirect

ISPRS Journal of Photogrammetry and Remote Sensing

journal homepage: www.elsevier.com/locate/isprsjprs

Prediction of L-band signal attenuation in forests using 3D vegetation structure from airborne LiDAR

Pang-Wei Liu [a,*], Heezin Lee [b,*], Jasmeet Judge [a], William C. Wright [c], K. Clint Slatton [b,d]

[a] Center for Remote Sensing, Agricultural and Biological Engineering Department, University of Florida, Gainesville, FL, USA
[b] Electrical and Computer Engineering Department, University of Florida, Gainesville, FL, USA
[c] United States Military Academy, West Point, NY, USA
[d] Civil and Coastal Engineering Department, University of Florida, Gainesville, FL, USA

ARTICLE INFO

Article history:
Received 1 November 2010
Received in revised form 26 April 2011
Accepted 26 April 2011
Available online 17 May 2011

Keywords:
Airborne LiDAR
Microwave attenuation
Remote sensing
GPS
3D vegetation structure

ABSTRACT

In this study, we propose a novel method to predict microwave attenuation in forested areas by using airborne Light Detection and Ranging (LiDAR). While propagating through a vegetative medium, microwave signals suffer from reflection, absorption, and scattering within vegetation, which cause signal attenuation and, consequently, deteriorate signal reception and information interpretation. A Fresnel zone enveloping the radio frequency line-of-sight is applied to segment vegetation structure occluding signal propagation. Return parameters and the spatial distribution of vegetation from the airborne LiDAR inside Fresnel zones are used to weight the laser points to estimate directional vegetation structure. A Directional Vegetation Density (DVD) model is developed through regression that links the vegetation structure to the signal attenuation at the L-band using GPS observations in a mixed forest in North Central Florida. The DVD model is compared with currently-used empirical models and obtained better R^2 values of 0.54 than the slab-based models. Finally, the model is evaluated by comparing with GPS observations of signal attenuation. An overall root mean square error of 3.51 dB and a maximum absolute error of 9.38 dB are found. Sophisticated classification algorithms and full-waveform LiDAR systems may significantly improve the estimation of signal attenuation.

1. Introduction

Microwave signals, especially at wavelengths of about 20 cm (L-band), have been extensively used in Global Positioning System (GPS) and wireless communications. However, these signals attenuate and cause loss in reception due to reflection, absorption, and scattering by the vegetation components, particularly in forested areas. Many studies have focused on understanding the propagation of microwave signals through vegetation canopy. For example, the Michigan Microwave Canopy Scattering (MIMICS) Model (Ulaby et al., 1990) is used to estimate the first-order signal backscattering coefficient and the signal attenuation. The MIMICS model is based upon the radiative transfer theory and requires knowledge of many vegetation parameters such as trunk height, foliage diameter, LAI, and dielectric properties of leaves. These parameters are typically obtained from either experiments or models. Since the forest canopy layer in the MIMICS model is assumed to be a stratified media, with homogeneous distribution over the crown volume, the estimates of signal attenuation would be highly correlated to the signal source elevation angle, θ. Bosisio and Dechambre (2004) found that the attenuation varies arbitrarily at the same θ, and concluded that the amount of foliage in the propagation path is a more important contributor than θ to the radar scattering and attenuation behavior for a vertical structure profile of foliage. Although θ may affect the attenuation at global scales, at the finer scales, most of the signal attenuation can still be predicted using different azimuth φ at the same θ.

In addition to the theoretical models, several empirical models have also been developed. The simplest ones use Beer's law to estimate the optical signal strength through a uniformly distributed, slab-like medium through an attenuation coefficient (Mätzler, 1994). The International Telecommunication Union (ITU) has also adopted several empirical models such as the Modified Exponential Decay (MED) (Weissberger, 1982; CCIR, 1986), Maximum Attenuation (MA), and Nonzero Gradient (NZG) (Seville and Craig, 1995) to estimate the signal attenuation between trees. In comparison to the theoretical models, these empirical models require fewer inputs, and the parameters in the empirical models are typically obtained from either linear or exponential regression. Savage et al.

* Corresponding authors. Address: Center for Remote Sensing, Agricultural and Biological Engineering Department, 280 Roger Hall, University of Florida, Gainesville, FL 32611, USA (P.-W. Liu); Electrical and Computer Engineering Department, 408 Reed Lab, University of Florida, Gainesville, FL 32611, USA (H. Lee). Tel.: +1 352 392 1864x280; fax: +1 352 392 1571.
E-mail addresses: bonwei@ufl.edu (P.-W. Liu), fields@ecel.ufl.edu (H. Lee).

0924-2716/$ - see front matter © 2011 International Society for Photogrammetry and Remote Sensing, Inc. (ISPRS). Published by Elsevier B.V. All rights reserved.
doi:10.1016/j.isprsjprs.2011.04.005

(2003) compared the estimates of signal attenuation from the models proposed by ITU with field measurements and found that the leaf state, geometry, and volume of biomass influenced the signal attenuation more significantly than tree species or leaf shape.

Studies indicate that foliage density and the signal propagation path that considers θ and ϕ simultaneously is critical for estimating the signal attenuation (Bosisio and Dechambre, 2004; Savage et al., 2003). Measuring foliage density in forested areas is laborious and time consuming. However, remote sensing technologies have been successfully applied to estimate the foliage parameters in forested areas. Two-dimensional passive remote sensing techniques such as satellite/aerial multispectral imaging or photography are capable of rapidly collecting forest information at larger spatial scales for estimating canopy density either directly (Newman, 1993; Jasinski, 1996) or indirectly from individual trees (Erikson, 2003). Such 2D studies represent the vegetation density in a top-to-bottom structural distribution without other directional characteristics. A 3D forest profile, on the other hand, considers the canopy density at different depths and can be used to account for the signal sources originating from all directions.

Airborne LiDAR systems are well-suited to obtain 3D observations from targets with high spatial accuracies because the point-to-point distances can be directly measured using scanning laser ranging technology. In addition, the laser pulses are capable of reaching the multiple layers of forest canopy and the ground due to the multiple returns obtained by LiDAR systems. In terms of the signal characteristics and data processing, LiDAR systems are categorized by return pulse information, resulting in either waveform, or discrete-returns and the width of the laser beam, resulting in different footprint sizes (Bortolot and Wynne, 2005). Generally, the full-waveform LiDAR systems have large footprints, with diameters of tens of meters, such as Laser Vegetation Imaging Sensor (LVIS) and Ice, Cloud and land Elevation Satellite (ICESat). The vertical profiles of forest structure can be densely sampled using these systems by finely digitizing the full waveform. Such systems have been applied to estimate biophysical parameters in forests (Lefsky et al., 1999; Weishampel et al., 2000; Harding et al., 2001; Ni-Meister et al., 2001; Drake et al., 2002a, 2002b; Duong et al., 2008). However, the pulse repetition rate is comparatively low in these systems which results in a much sparser horizontal point spacing than small-footprint systems. Thus, the full-waveform systems with large footprints are less applicable for fine scale estimation of forest structure. Recently, full-waveform systems have been developed with smaller footprints, with diameters of 20–30 cm. Although these systems provide large quantities of data that are more difficult to process (Evans et al., 2009; Mallet and Bretar, 2009), a few studies have shown their potential for object classification (Kirchhof et al., 2008; Alexander et al., 2010) and tree segmentation (Reitberger et al., 2009).

Due to dense samples obtained by the discrete-return systems with their small footprints, Clark et al. (2004) found that these systems were appropriate in ecological studies such as tracking tree-fall gap dynamics and scaling point-based data to broader scale (i.e. mapping). Such systems require extraction of ground surface to estimate vegetation characteristics. Earlier studies focused on ground surface extraction have used morphological or statistical probability filters to segment ground points and vegetation points (Clark et al., 2004; Kampa and Slatton, 2004; Meng et al., 2009). With the development of the scanner technology, the discrete return systems have been employed to estimate canopy structure and biophysical parameters of trees (Palenichka and Zaremba, 2007; Wang et al., 2008; Hosoi and Omasa, 2009; Lee et al., 2010). Such 3D estimation allows measurement of the directional vegetation structure for estimating signal attenuation. For example, the canopy height can be used as the vegetation depth in the slab model, which simulates the vegetation as a uniformly distributed layer. A slab model is simple, lacking heterogeneous of vegetation structure. Swanson et al. (2009) used such a model in conjunction with LiDAR observations to estimate the path lengths between a transmitter and a receiver through foliage and stem in coniferous forests. The path lengths were related to attenuation in the signal from a Synthetic Aperture Radar (SAR) at UHF using first degree polynomial with two variables to account for the attenuation by foliage and stem. Although the model accounted for the directional path length through the vegetation, the vegetation volume density within the path length was the same in all directions. In this study, we propose a novel model to account for the vegetation density along the line of sight using LiDAR observations.

The goal of this study is to estimate the attenuation of microwave signals in forests using observations from an airborne discrete-return LiDAR system and the GPS. The objectives of this study are to (1) derive mean tree height using LiDAR measurements, (2) segment the vegetation structure along the line of sight using the Fresnel zone and using a weighting scheme to account for different levels of attenuation by the vegetation, (3) develop a Directional Vegetation Density (DVD) model with linear and exponential regressions and compare its predictions to the slab model at three GPS training sites, (4) validate the model providing the best R^2 values with the GPS observations at the fourth site. Because the DVD model requires fewer parameters than the theoretical models, and accounts for the heterogeneous vegetation structure in both θ and φ, the methodology developed in this study can be used to estimate the coverage and quality of signal reception in other forested regions.

2. Study region and remote sensing observations

2.1. Study region

This study was conducted in the Hogtown Forest located in North-Central Florida, USA (29°39′N, 82°22′W). The forest is a natural forest consisting of mixed species of vegetation with about 80% deciduous trees, such as oak, white ash, maple, etc., and 20% coniferous trees, such as loblolly pine, cypress, etc. The average height of the trees in the region is 35 m and the trees consist of multiple layers of foliage with an abundant understory and varied tree spacing. The topography in this region is very flat with ground elevations varying as little as 2 m, minimizing the effects of terrain for this study. Fig. 1 shows a sample of the study site with its location. Airborne LiDAR observations were obtained for the entire study region. The GPS observations were conducted at four sites within the region, differing in vegetation complexity. Observations at three sites, shown in Fig. 1(b), were used for developing the slab and the DVD models and those at the fourth site were used to evaluate the best model. The site 1 consisted of sparser foliage with fewer stems, the site 2 consisted of denser foliage with significant closure and more stems, and the site 3 consisted of the densest foliage with almost complete closure and large tree trunks around the receiver, as shown in Fig. 2((a)–(c)), respectively. The vegetation structure at site 4 was similar to that at site 2. Additional GPS observations were conducted on an open roof structure serving as a reference station.

2.2. GPS observations

GPS observations were conducted on December 12, 2008, using an Ashtech Z-surveyor receiver of geodetic quality and Marine L1–L2 antennae. The system has a uniform gain for all signals between the elevations of 15° and 90° (Sabatini and Palmerini, 2008) and the setup enables easy detection of GPS carrier signals. Every receiver antenna was mounted on a tripod at a height of 1.5 m to avoid interference from forest understory. At each of the three GPS sites,

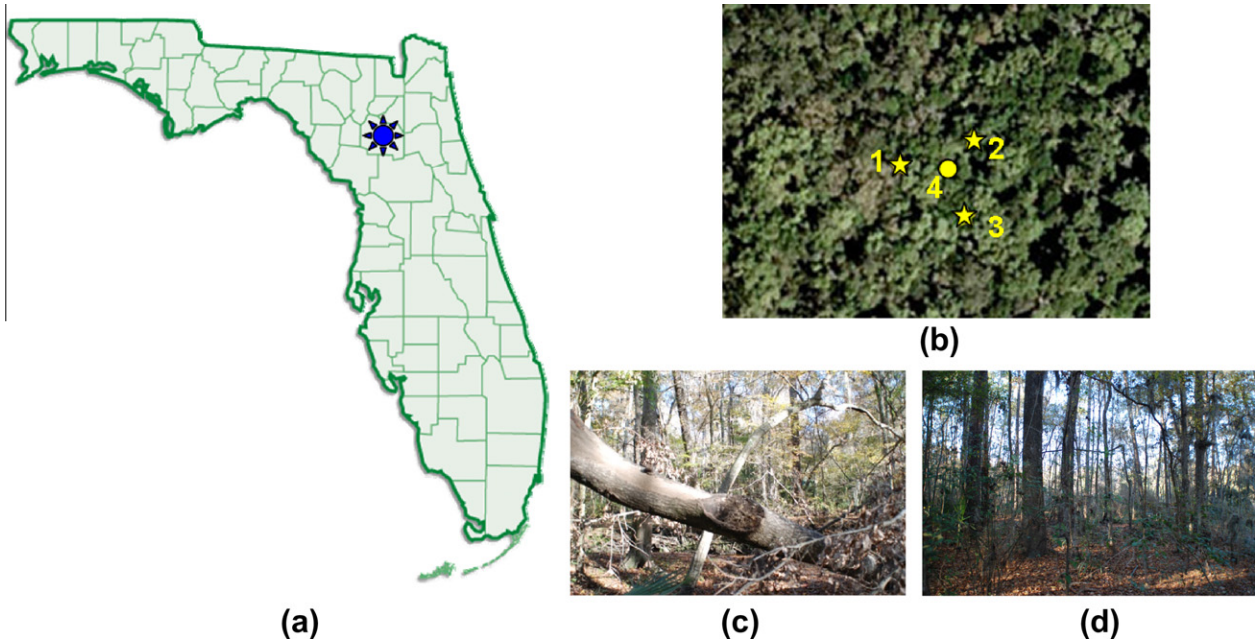

Fig. 1. (a) The location of the Hogtown forest near Gainesville, FL, (b) an aerial photograph of the Hogtown forest and the location for the site locations for the GPS observations, (c) a typical scene showing the under canopy vegetation interference and (d) the uneven distribution of stems in the forest.

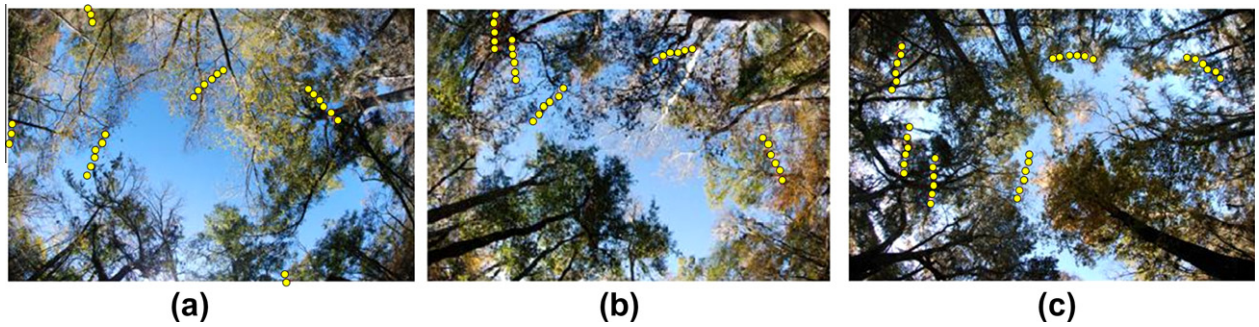

Fig. 2. Fisheye lens photos at the three sites, with circles showing the SV trajectories. (a) site 1, (b) site 2, and (c) site 3.

the data were obtained for over 40 min at recording rate of 0.1 Hz, resulting in >1200 observations. Fig. 2 shows fisheye lens images with the GPS trajectories and rates of signal attenuation at the three sites. At the fourth site, the GPS observations were obtained for 5 h at the same recording rate. In addition to the observations at the four locations in the Hogtown Forest, another receiver antenna was located under open sky conditions on a roof-top of Weil Hall at the University of Florida (UF), located within 3 km of the study region. This set up served as a reference station.

The GPS recorded observations in the format of National Marine Electronic Association (NMEA) messages and provided signal to noise ratio (SNR) of each space vehicle (SV), with its directional locations (θ, φ) and the position solutions of GPS sites. For a geodetic quality receiver, such as the one used in this study, the environmental noise is constant and the SNR is proportional to the strength of the GPS signal (Bilich et al., 2004). Even though the signal strength measured by the GPS receivers is mainly influenced by canopy foliage, spatial and temporal averaging is necessary to mitigate local variations in the canopy cover fraction, due to wind, etc. (Ulaby et al., 1986). Locating exact position of the SV is also challenging because the SVs are moving sources at 0.5°/min. NMEA messages provide the directional position (θ, φ) in degrees. In this study, the instant location of a SV is estimated using the median value for six minutes of GPS data, assuming ±1° error bearing in the system. The signal attenuation induced by vegetation was then deduced by subtracting the SNR in forest from the SNR at the open reference station.

2.3. LiDAR observations

Airborne LiDAR observations were conducted using the UF Airborne Laser Swath Mapping (ALSM) system (Carter et al., 2001) on December 9, 2008, 3 days before the GPS observations. The system is integrated with a GPS and an inertial measurement unit (IMU), and mounted on a twin-engine Cessna 337 Skymaster. It provides laser pulse rates of up to 167 kHz, with up to 4 returns/transmitted pulse, intensities of each return, and two beam divergences of 0.25 and 0.80 mrad. Accurate geo-locations of returns from each transmitted pulse are determined by differential GPS and the intensities of returns reflect at the near-IR wavelength of 1064 nm. The LiDAR data in this study were acquired at a pulse repetition rate of 125 kHz, a beam divergence of 0.25 mrad, a scan rate of 45 Hz, a scan angle range of ±15°, and an average height of 600 m above ground level. Thus, the pulse density is about 4 pulses/m^2. By overlapping adjacent vertical and horizontal swaths by 50%, an average pulse density of about 16 pulses/m^2 was obtained. Such overlapping was necessary to ensure complete coverage of the study region. However, combining multiple swaths causes an uneven

distribution of LiDAR points on the scanning targets, resulting in an incorrect estimation of vegetation density from distribution of LiDAR points. A simple normalization process was applied to mitigate this effect. It involved gridding the experimental region into 1 m × 1 m cells and normalizing the LiDAR points inside each cell by the number of swaths covering the cell.

3. Methodology

3.1. Estimation of vegetation structure

3.1.1. Estimation of vegetation height using LiDAR observation

The nominal path length through a uniformly distributed vegetation was computed for estimating signal attenuation in the slab model. An adaptive multiscale filter developed by Kampa and Slatton (2004) was employed to classify ground points from the LiDAR observations. The mean tree height, 35 m, in the Hogtown Forest was directly estimated by subtracting the bare ground surface height from the canopy top height.

3.1.2. Segmentation of vegetation using Fresnel zone

To estimate signal interference, it is critical to account for not only the obstructions along the line of sight, but also a region around the line of sight inside which the signal is impacted the most by absorption, reflection, and scattering. Typically, conical and cylindrical shaped regions are most commonly employed to segment the obstruction along the line of sight vector (Wright et al., 2008; Lee et al., 2009), with size of the regions determined empirically. In wireless communications, a Fresnel zone has been applied to evaluate the obstruction between the transmitter and receiver (Smith, 1993; Cash, 2003). As shown in Fig. 3(a), a Fresnel zone surrounding the line of sight vector defines a circular region as a function of distance between the transmitter and the receiver. Objects inside the region interfere with the signal propagation. The general equation for estimating the Fresnel zone is (Smith, 1993):

$$F_n = \sqrt{\frac{n\lambda d_1 d_2}{d_1 + d_2}} \tag{1}$$

where F_n is the radius of the nth order Fresnel zone at a location, K, along the line of sight in m, d_1 is the distance from the transmitter to K in m, d_2 is the distance from the receiver to K in m, and λ is the wavelength of the transmitted signal in m. In this study, the signal sources were GPS SVs, so their line of sight vectors centered at the receiver antenna of the SVs, as shown in Fig. 3(b). Because of SVs' high altitudes, $d_2 \gg d_1$, the Eq. (1) can be simplified as

$$F_n = \sqrt{n\lambda d_1} \tag{2}$$

In general, obstructions inside the 1st order of the Fresnel zone strongly impact the signal transmission, while those inside the higher order zones are less impacting. Only the LiDAR points falling inside the 1st order zone were considered in this study.

3.1.3. Weighting scheme for estimating vegetation density

Signal obstruction by an object depends upon its size, reflectivity, and location. In this study, we used a weighting scheme that accounted for the above characteristics of attenuating objects. These effects were assumed statistically independent, so the weighted point density of the vegetation inside the Fresnel zone, $P(\theta, \phi)$, is calculated as follows:

$$P(\theta,\phi) = \sum_{i=1}^{N} w_{ri} \cdot w_{di} \cdot w_{\theta_{div^i}} \tag{3}$$

where N is the total number of LiDAR points inside the Fresnel zone, w_{ri} is the weight of the ith point based upon the order of the LiDAR returns, w_{di} is the weight of the ith point based upon the distance from the GPS receiver to the point, and $w_{\theta_{div^i}}$ is the weight of the ith point based upon the divergence of the point from the line of sight.

3.1.3.1. Weights based upon return order, w_r. The return order of the LiDAR pulses depend upon the distance of the target from the LiDAR system, and the intensities of the returns depend upon the reflective properties and the size of the target. In the absence of detailed structure, the vegetation at the sites are assumed to have three layers, with upper and mid canopy layers, and an understory layer, primarily consisting of tree trunks and minimal shrubbery. Following Meir et al. (2000) and the fisheye lens images of our sites (see Fig. 2), the distribution of leaf density is assumed to be sparser in the top canopy and denser in the mid canopy layer. Hence, the leading edge of the laser results in multiple returns, with earlier returns obtained from a sparser canopy, while later returns from a denser canopy. Furthermore, the weights are normalized to ensure that the less dense vegetation is assigned a lower value of w_r than the denser vegetation. In this study, the sum of w_r's of all returns

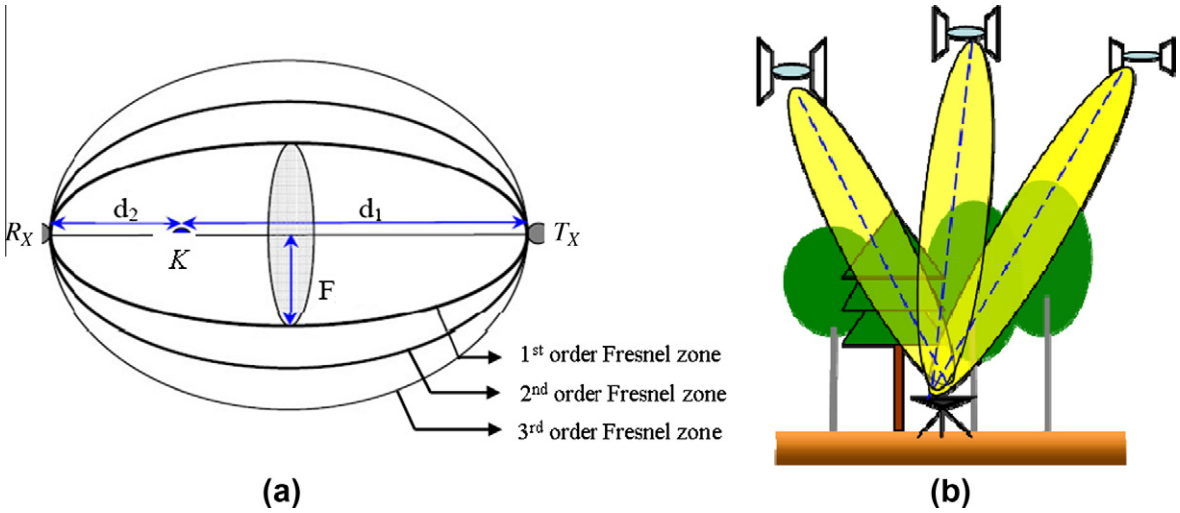

Fig. 3. (a) The shape and orders of Fresnel zone, where T_x and R_x are the receiver and the transmitter, d_1 and d_2 are the distances between location K and the transmitter and receiver, respectively, and F is the radius of Fresnel zone, and (b) the Fresnel zone aiming at the SVs for this study.

from each pulse is 4, following the four possible returns using our LiDAR system.

The weight assignments are shown in Fig. 4. A single return occurs most likely when the laser pulse hits either the denser middle layer of the canopy, tree trunk, or ground, as shown in Fig. 4(a). Such targets reflect all the transmitted energy so the highest normalized weight of 4 is assigned in this case. In the case of two returns, the first return is most likely from the top layer with lower density than the middle layer, and the second return is likely from either the denser mid canopy, tree trunk, or ground, as shown in Fig. 4(b). The weight of the second return ($w_2 = 3$) is lower than weights of 4 in the single return case because of the decreased energy associated with the second return even though possibly both could be from an equally dense target. Similarly, in the case of three returns, the first return is assigned a weight of 1 because it was most likely obtained from the top canopy layer. In our study, 69% of the third returns were from 0 to 20 m above the ground, primarily occupied the trunks. Hence, the third return is assigned a higher weight than the second return that was most likely from a sparser mid canopy, with $w_2 = 1$ and $w_3 = 2$. However, in the case of four returns, the first three returns are assigned a weight of 1, while the assignment of the fourth return is challenging given the LiDAR system used in this study is limited to four returns. The last return could be from either a dense target such as the trunk, the ground, or from a sparser target as shown in Fig. 4(d). Hence, without further knowledge into the origin of the last return, we assigned all returns equal weights. In our study, the last return is assigned a weight of 1, assuming it is from the branches or foliage. This may slightly underestimate the attenuation. However, in our case, only 0.8% of the total points were fourth returns, not including the returns from the ground. More sophisticated classification algorithms are needed to understand the vegetation characteristics for developing more robust algorithm for assigning w_r.

3.1.3.2. Weights based upon the distance between the GPS receiver and the vegetation point, w_d. Generally, objects farther from the receiver contribute less toward signal attenuation. The w_d varies between 0 and 1, decreasing monotonically with the distance (Lee et al., 2009):

$$w_d = \frac{(d - d_{\max})^2}{d_{\max}^2} \tag{4}$$

where d is the distance between the vegetation point and the receiver, obtained from the LiDAR, and $d_{\max}$ is the maximum distance beyond which the point is non-attenuating. When the object is at the receiver, $d = 0$, it causes maximum attenuation, and $w_d = 1$. When the object is far away, $d \geqslant d_{\max}$, and $w_d = 0$. In this study, $d_{\max} = 150$ m, based upon the mean tree high of 35 m and the minimum elevation angle for the GPS SV of 15° as shown in Fig. 5.

3.1.3.3. Weight based upon the divergence of the vegetation point from line of sight, $w_{\theta_{div}}$. The signal attenuation due to the angular divergence of vegetation point from line of sight was assumed normally distributed within the Fresnel zone as follows:

$$W_{\theta_{div}} = \frac{a}{\sigma\sqrt{2\pi}} \exp\left(-\frac{x^2}{2\sigma^2}\right); \quad x = \frac{\theta_{div}}{\theta_{div_{\max}}} \tag{5}$$

where x is the normalized angular divergence of the vegetation point, θ_{div} is the angle of divergence of the point from line of sight vector, $\theta_{div_{\max}}$ is the maximum angle of divergence at the boundary of the Fresnel zone, as shown in Fig. 5. The variance σ^2 and the scalar parameter a are set to 0.6185 and 0.6450, respectively, in this study. A vegetation point located on the line of sight vector is assigned the maximum of $w_{\theta_{div}} = 1$ and a point at the edge of the Fresnel zone is assigned the minimum weight, empirically determined to be 0.3, for the study.

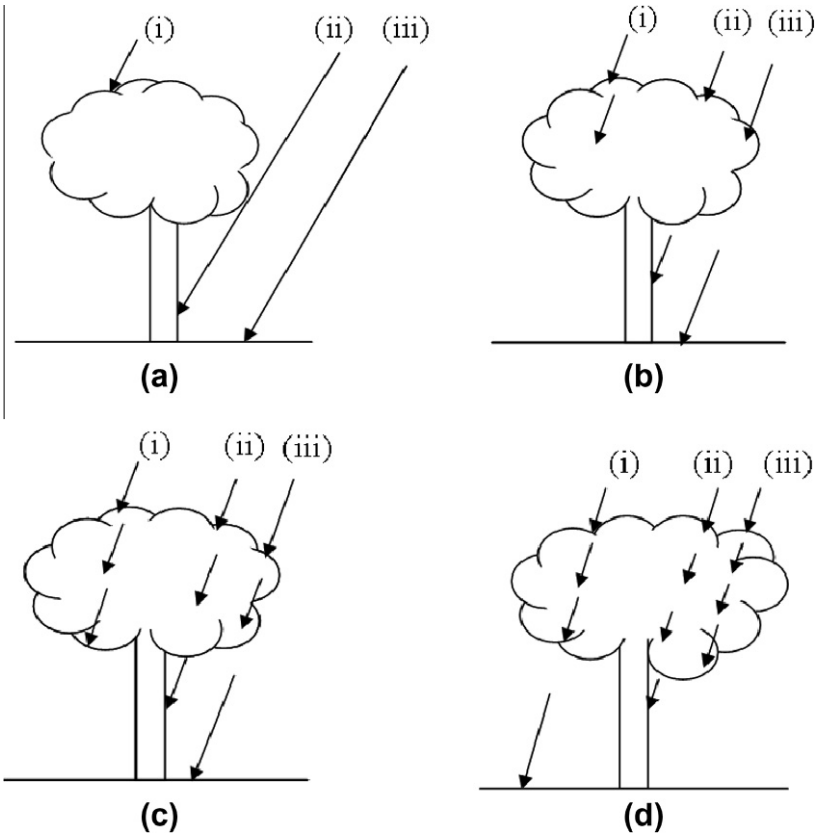

Fig. 4. Assignment of the weight, w_r, for each vegetation point based upon the order of the LiDAR returns, (a) the single return case with $w_1 = 4$, (b) the two return case with $w_1 = 1$ and $w_2 = 3$, (c) the three return case with $w_1 = w_2 = 1$ and $w_3 = 2$, and (d) the four return case with $w_1 = w_2 = w_3 = w_4 = 1$.

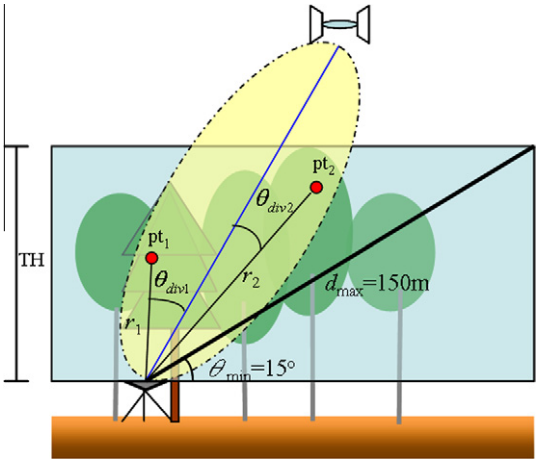

Fig. 5. Estimates of w_d and $w_{\theta_{div}}$ based upon the distance and the divergence angle. TH is the tree height, d_{max} is the max distance, r_1 and r_2 are the distances from the GPS receivers to vegetation points pt_1 and pt_2; θ_{div1} and θ_{div2} are the divergences of pt1 and pt2 from line of sight.

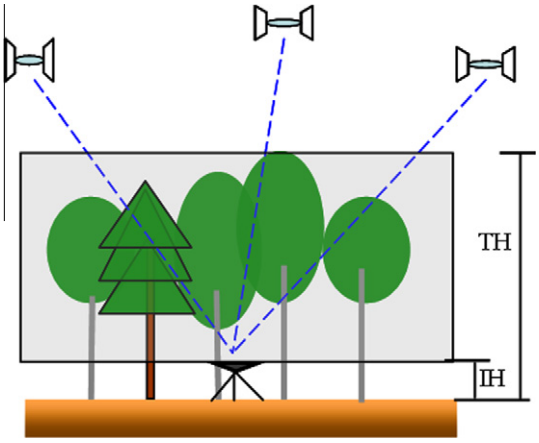

Fig. 6. Illustration of the vegetation slab model. IH is the height of the GPS receiver and TH is mean tree height from the ground surface.

3.2. Models for microwave signal attenuation

3.2.1. Slab model

Slab type models based upon the Beer's law and Modified Exponential Decay (MED) (Weissberger, 1982) relate the nominal signal path length within the uniformly distributed vegetative medium to the observed signal attenuation using linear or exponential functions, as shown in Eqs. (6) and (7), respectively:

$$L(\theta) = A \cdot d(\theta) + \beta \tag{6}$$

$$L(\theta) = B \cdot d^{Z}(\theta) \tag{7}$$

where $L(\theta)$ is the signal attenuation of an SV at θ in dB, nominal path length $d(\theta) = h/\sin(\theta)$, where h is the estimated tree height from Section 3.1.1, also shown in Fig. 6. The parameters A, β, B, and Z are estimated through regression using a least square adjustment.

3.2.2. Directional Vegetation Density (DVD) Model

In this study, we present a DVD model, where the DVD, also called the vegetation point density, within a Fresnel zone is related to the observed signal attenuation from each SV through linear or exponential functions, as shown in Eqs. (8) and (9), respectively.

$$L(\theta, \phi) = C \cdot P(\theta, \phi) + D \tag{8}$$

$$L(\theta, \phi) = E \cdot P^{F}(\theta, \phi). \tag{9}$$

where $L(\theta, \phi)$ is the signal attenuation as in the previous equations, $P(\theta, \phi)$ is the weighted point density obtained from Eq. (3). The parameters C, D, E, and F are estimated using a least square adjustment.

4. Results and discussion

In this section, we discuss the impacts of the weighting scheme on signal attenuation, compare the performance of the slab and the DVD models using linear and exponential equations, and present the effectiveness of multiple swath observations by the LiDAR for estimation of signal attenuation.

4.1. Impact of weighting scheme

To evaluate the weighting scheme, we compared the linear and the exponential DVD models with and without the weighting scheme. When the vegetation points are not weighted, all the points inside the Fresnel zone are weighted equally, so that $P(\theta, \phi)$ is the total number of points in the zone. As shown in Tables 1 and 2, the R^2 values at sites 1 and 2 do not show significant increase when the weighting scheme is used. This is primarily because the vegetation at the two sites is less dense, without much understory. However, at site 3, the weighting scheme performs better, with an increase in R^2 values of 0.23 and 0.08 for the linear and exponential models, respectively. The vegetation at site 3 was

Table 1
The regression results of linear and exponential DVD models.

GPS sites	Linear-DVD model				Exponential-DVD model			
	Eq.	R^2	RMSE	MAE	Eq.	R^2	RMSE	MAE
Site 1	$L = 0.0514P + 2.7873$	0.6596	2.26	4.93	$L = 0.3815P^{0.6614}$	0.7306	2.20	4.93
Site 2	$L = 0.0489P + 2.7459$	0.5504	2.35	5.68	$L = 0.7478P^{0.5640}$	0.5640	2.44	5.64
Site 3	$L = 0.0480P + 2.0033$	0.6072	2.77	7.59	$L = 0.2355P^{0.7153}$	0.3799	2.95	8.02
All sites	$L = 0.0477P + 2.6627$	0.5956	2.53	7.36	$L = 0.5088P^{0.5766}$	0.4770	2.64	7.07

Table 2
The regression results of linear and exponential DVD models without weighing scheme.

GPS sites	Linear-DVD model				Exponential-DVD model			
	Eq.	R^2	RMSE	MAE	Eq.	R^2	RMSE	MAE
Site 1	$L = 0.0149P + 4.6356$	0.5815	2.55	5.33	$L = 0.6290P^{0.4825}$	0.7248	2.27	5.50
Site 2	$L = 0.0264P + 2.7315$	0.5744	2.28	5.29	$L = 0.4580P^{0.5354}$	0.5794	2.35	5.31
Site 3	$L = 0.0249P + 3.5103$	0.3718	3.51	7.92	$L = 0.3412P^{0.5917}$	0.2993	3.58	8.38

Table 3
The regression results of linear and exponential slab models.

GPS sites	Linear slab model				Slab model – exponential			
	Eq.	R^2	RMSE	MAE	Eq.	R^2	RMSE	MAE
Site 1	$L = 0.1083d + 0.9175$	0.5241	2.68	7.20	$L = 0.1082d^{1.0164}$	0.5258	2.72	7.26
Site 2	$L = 0.1634d - 2.5059$	0.4995	2.47	5.42	$L = 0.0192d^{1.4312}$	0.478	2.53	5.96
Site 3	$L = 0.0732d + 3.7508$	0.0797	4.24	10.13	$L = 0.4350d^{0.6762}$	0.0851	4.42	11.42

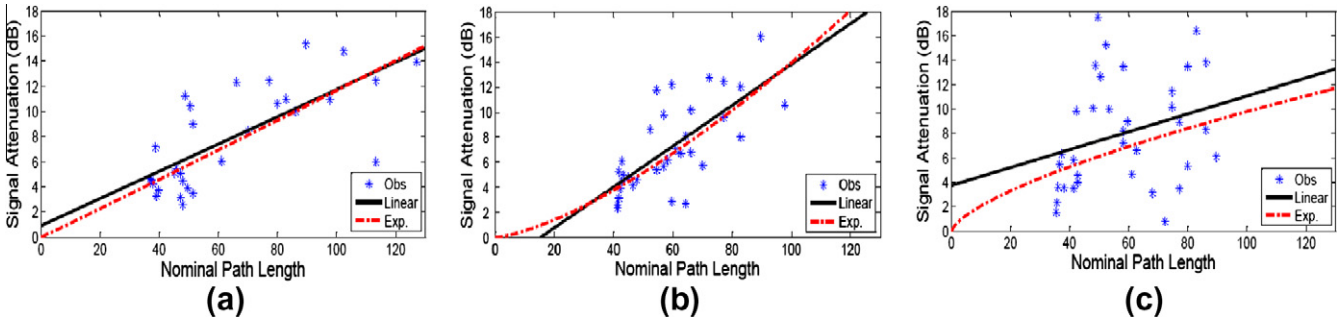

Fig. 7. Signal attenuation as a function of nominal path length and the regression of the linear and exponential slab model at (a) site 1, (b) site 2, and (c) site 3.

more complex with significant understory, resulting in a strong dependence of signal transmission upon the heterogeneous vegetation structure.

Although our weighting scheme for the four returns may result in slight underestimation in the attenuated signal, in this study, only 0.8% of total 3,746,455 points were fourth returns and non-ground points. For the improved estimation of signal attenuation, more robust algorithms, such as stem point clustering (Reitberger et al., 2009), are needed to better understand the vegetation characteristics. In addition, the full-waveform LiDAR systems provide better vertical distribution of vegetation and may also be used.

4.2. Comparison of slab and DVD models

As shown in Table 3 and Fig. 7, the linear and the exponential slab models provide better estimates of signal attenuation at site 1 than at site 3, by an R^2 value of 0.44 and RMSE of about 1.6 dB. Because the vegetation distribution at site 3 is more complex and azimuthally heterogeneous, the slab models, which assume homogeneity of the vegetation distribution, are unable to provide accurate estimates of signal attenuation.

As shown in Table 1 and Fig. 8, the linear DVD model performs better than the linear slab model, with the increase in R^2 values of

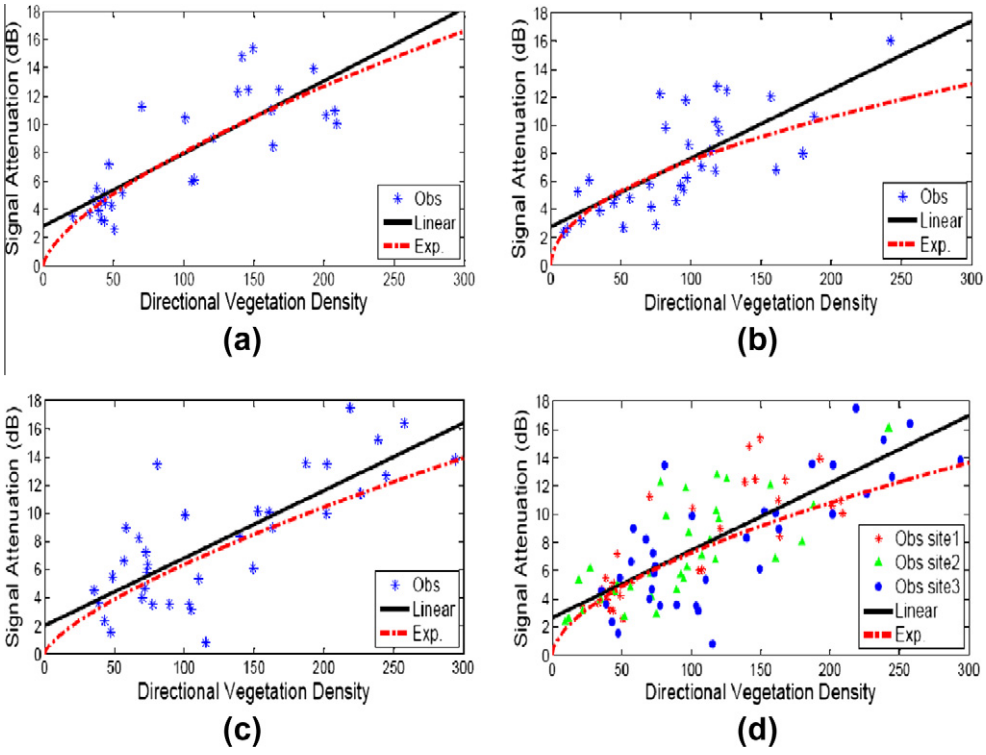

Fig. 8. Signal attenuation as a function of Directional Vegetation Density (DVD) and the regression of the linear and exponential DVD models at (a) site 1, (b) site 2, (c) site 3, and (d) combination of all three sites.

0.14, 0.05, and 0.54 at the three sites, respectively. The exponential DVD model provides better R^2 values by 0.21, 0.09, and 0.30 than the exponential slab models for the three sites, respectively. As per our hypothesis, the DVD models perform significantly better than the slab models at site 3, where the vegetation structure is complex and heterogeneous, so both vegetation density and azimuthal dependence are important for accurate and robust estimation of signal attenuation.

The DVD models were also developed combining observations from all the three training sites. As shown in Table 1, the linear DVD model obtains a higher R^2 value by 0.12 than the exponential model. In addition, the linear model provides similar R^2 values for the three sites, indicating the stability of the model compared to the exponential model. In the following section, we validate only the linear DVD model.

4.3. Validation of the linear DVD model

The signal attenuation estimated by the DVD model was compared with those obtained using the GPS observations, with a receiver at the fourth site and eleven orbiting SVs. The overall RMSE using the eleven SV observations is 3.51 dB. In Fig. 9((a)–(e)), we show the trajectories and the time series comparison with four of the 11 SVs that had longer trajectories: SV trajectories: SV11, SV17, SV27, and SV28. The RMSEs between the model estimates and the GPS observations of signal attenuation of the four SVs are 3, 4, 2, and 4 dB, respectively. The model estimates are farthest from the SV17 and SV28 observations by about 5–8 dB, as shown in Fig. 9(c) and (e). This is primarily because of the big tree trunks severely blocking the signal at site 4, as the SV passed by (see Fig. 9(a)). This indicates that in spite of high spatial resolution, the ALSM system, with 4 returns/pulse used in this study, undersampled the understory vegetation structure, including the tree trunk under a dense canopy. Most previous studies (Violette et al., 1983; Ulaby et al., 1986; Bosisio and Dechambre, 2004) indicated that the leaves impact signal attenuation more than the stems, however, for estimating the signal attenuation with finer spatial resolution, big trunks may have a significant impact on signal attenuation. Future studies may need to have *a priori* knowledge of the understory structure either from individual tree

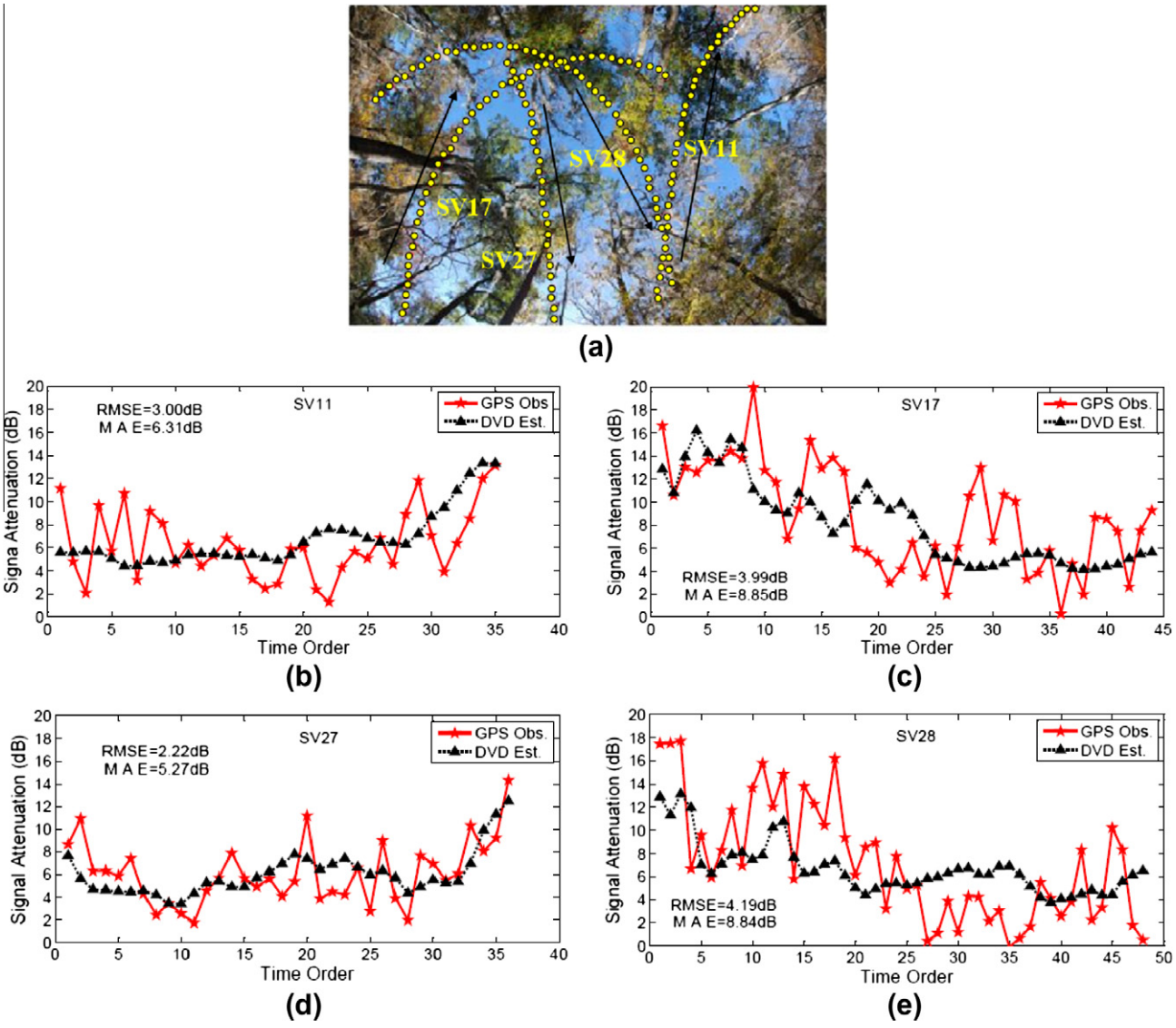

Fig. 9. (a) The fisheye lens photo showing trajectories of the SVs at site 4. The comparison of time series of signal attenuation estimated by the linear DVD model with those observed by the four SVs (b) SV11; (c) SV 17; (d) SV27, and (e) SV28. Each SV observation in the figures represents signal attenuation averaged over 6 min. RMSE = root mean square error. MAE = maximum absolute error.

Table 4
The regression results of linear and exponential DVD models from single swath LiDAR observations.

GPS sites	Linear-DVD model (one swath)				Exponential-DVD model (one swath)			
	Eq.	R^2	RMSE	MAE	Eq.	R^2	RMSE	MAE
Site 1	$L = 0.0528P + 2.7355$	0.6671	2.24	4.69	$L = 0.4038P^{0.6518}$	0.7488	2.16	4.76
Site 2	$L = 0.0507P + 2.8756$	0.5558	2.33	5.47	$L = 0.7944P^{0.4945}$	0.5727	2.41	5.44
Site 3	$L = 0.0525P + 1.6782$	0.5860	2.85	7.65	$L = 0.3412P^{0.5917}$	0.3541	3.04	8.12

detection or biomass estimation models for an improved prediction of signal attenuation using LiDAR. In addition, full-waveform systems with smaller footprints may be used to obtain the full vertical structure of the vegetation.

4.4. Comparison of single and multiple swaths

Observations from multiple swaths are usually necessary to obtain complete coverage of the region of interest or to enhance description of the region from different views. However, the computational demands increase as the number of swaths increases. We compared the linear DVD model using $P(\theta, \phi)$ values obtained from multiple swaths with those that were obtained from a single swath to understand the impact of the number of swaths on estimation of signal attenuation. As shown in Tables 1 and 4, the differences of R^2 values from both methods are similar, within 0.02, implying that the multiple LiDAR observations used in this study obtain similar quality of data set as the single swath for extracting the vegetation structure.

5. Conclusion

In this study, a methodology integrating the communication theory and LiDAR observations is proposed to estimate L-band signal attenuation from GPS observations in forests. Although the slab models provide moderate estimation of signal attenuation if the vegetation is distributed uniformly, their application is limited in the forested regions due to significant heterogeneity in vegetation structure. The DVD model considers the weighted vegetation structure inside a region around signal path. A comparison of the model with and without the weighting scheme indicated that the scheme has a significant impact on signal attenuation estimates at the site with denser and heterogeneous vegetation. The linear DVD model was the most stable and obtained the best R^2 of 0.6072 for the most complex site. This study demonstrates that both the vegetation density and azimuthal dependence are important for accurate estimation of signal attenuation. The overall estimation of signal attenuation from the linear DVD model matched well with the GPS observations with a RMSE of 3.51 dB. The vegetation structure in the understory could not be well-sampled by discrete return LiDAR system and resulted in an underestimation of signal attenuation by about 5–8 dB. *A priori* knowledge of the vegetation structure by sophisticated classification algorithms and the full-waveform LiDAR will significantly improve the estimation of signal attenuation using LiDAR observations.

Acknowledgements

This work was partially supported by the National Science Foundation (NSF) through the National Center for Airborne Laser Mapping (NCALM) under Grant EAR-0518962 and the US Army Research Office (ARO) under Grant W911NF-06-1-0459. The authors thank the anonymous reviewers for their helpful comments and suggestions.

References

Alexander, C., Tansey, K., Kaduk, J., Holland, D., Tate, N.J., 2010. Backscatter coefficient as an attribute for the classification of full-waveform airborne laser scanning data in urban areas. ISPRS Journal of Photogrammetry and Remote Sensing 65 (5), 423–432.

Bilich, A., Larson, K.M., Axelrad, P., 2004. Observations of signal-to-noise ratios (SNR) at geodetic GPS site CASA: Implications for phase multipath. Proceedings of the Center for European Geodynamics and Seismology 23, 77–83.

Bortolot, Z.J., Wynne, R.H., 2005. Estimating forest biomass using small footprint LiDAR data: an individual tree-based approach that incorporates training data. ISPRS Journal of Photogrammetry and Remote Sensing 59 (6), 342–360.

Bosisio, A.V., Dechambre, M., 2004. Predictions of microwave attenuation through vegetation: a comparison with measurements. International Journal of Remote Sensing 25 (19), 3973–3997.

Carter, W.E., Shrestha, R., Tuell, G., Bloomquist, D., Sartori, M., 2001. Airborne laser swath mapping shines new light on earth's topography. EOS, Transactions, American Geophysical Union 82 (46), 549, 550, 555.

Cash, J.M., 2003. Using light detection and ranging (LiDAR) imagery to model radio wave propagation. Master Thesis, Virginia Polytechnic Institute and State University, Blacksburg, VA.

Clark, M.L., Clark, D.B., Roberts, D.A., 2004. Small-footprint LiDAR estimation of sub-canopy elevation and tree height in a tropical rain forest landscape. Remote Sensing of Environment 91 (1), 68–89.

Duong, H., Pfeifer, N., Lindenbergh, R., Vosselman, G., 2008. Single and two epoch analysis of ICESat full-waveform data over forested areas. International Journal of Remote Sensing 29 (5), 1453–1473.

Drake, J.B., Dubayah, R.O., Clark, D.B., Knox, R.G., Blair, J.B., Hofton, M.A., Chazdon, R.L., Weishampel, J.F., Prince, S.D., 2002a. Estimation of tropical forest structural characteristics using large-footprint lidar. Remote Sensing of Environment 79 (2–3), 305–319.

Drake, J.B., Dubayah, R.O., Knox, R.G., Clark, D.B., Blair, J.B., 2002b. Sensitivity of large-footprint lidar to canopy structure and biomass in a neotropical rainforest. Remote Sensing of Environment 83 (2–3), 378–392.

Erikson, M., 2003. Segmentation of individual tree crown in closure aerial photographs using region growing supported by Fuzzy rules. Canadian Journal of Forest Research 33 (8), 1557–1563.

Evans, J.S., Hudak, A.T., Faux, R., Smith, A.M.S., 2009. Discrete return lidar in natural resources: recommendations for project planning, data processing, and deliverables. Remote Sensing 1 (4), 776–794.

Harding, D.J., Lefsky, M.A., Parker, G.G., Blair, J.B., 2001. Laser altimeter canopy height profiles methods and validation for close-canopy, broadleaf forests. Remote Sensing of Environment 76 (3), 283–297.

Hosoi, F., Omasa, K., 2009. Estimating vertical plant area density profile and growth parameters of wheat canopy at different stages using three-dimensional portable lidar imaging. ISPRS Journal of Photogrammerty and Remote Sensing 64 (2), 151–158.

International Radio Consultative Committee (CCIR), 1986. Influences of terrain irregularities and vegetation on tropospheric propagation. Reports and recommendations of the CCIR, 236-6, Geneva.

Jasinski, M.F., 1996. Estimation of subpixel vegetation density of natural regions using satellite multispectral imagery. IEEE Transactions on Geoscience and Remote Sensing 34 (3), 804–813.

Kampa, K., Slatton, K.C., 2004. An adaptive multiscale filter for segmentation vegetation in ALSM data. In: Proceedings of IEEE International Geoscience and Remote Sensing Symposium (IGARSS), vol. 6, pp. 3837–3840.

Kirchhof, M., Jutzi, B., Stilla, U., 2008. Iterative processing of laser scanning data by full waveform analysis. ISPRS Journal of Photogrammetry and Remote Sensing 63 (1), 99–114.

Lee, H., Slatton, K.C., Roth, B.E., Cropper Jr., W.P., 2009. Prediction of forest canopy light interception using three-dimensional airborne LiDAR data. International Journal of Remote Sensing 30 (1), 189–207.

Lee, H., Slatton, K.C., Roth, B.E., Cropper Jr., W.P., 2010. Adaptive clustering of airborne LiDAR data to segment individual tree crown in managed pine forests. International Journal of Remote Sensing 31 (1), 117–139.

Lefsky, M.A., Cohen, W.B., Acker, S.A., Parker, G.G., Spies, T.A., Harding, D., 1999. LiDAR remote sensing of the canopy structure and biophysical properties of Douglas-fir western hemlock forests. Remote Sensing of Environment 70 (3), 339–361.

Mallet, C., Bretar, F., 2009. Full-waveform topographic lidar: state-of-the art. ISPRS Journal of Photogrammetry and Remote Sensing 64 (1), 1–16.

Mätzler, C., 1994. Microwave transmissivity of a forest canopy: experiments made with a beech. Remote Sensing of Environment 48 (2), 172–180.
Meir, P., Grace, J., Miranda, A.C., 2000. Photographic method to measure the vertical distribution of leaf area density in forests. Agricultural and Forest Meteorology 102 (2–3), 105–111.
Meng, X., Wang, L., Silván-Cárdenas, J.L., Currit, N., 2009. A multi-directional ground filtering algorithm for airborne LiDAR. ISPRS Journal of Photogrammetry and Remote Sensing 64 (1), 117–124.
Newman, A.P., 1993. Monitoring urban forest canopy cover using satellite imagery. Environmental Monitoring and Assessment 26 (2–3), 175–176.
Ni-Meister, W., Jupp, D.L.B., Dubayah, R.O., 2001. Modeling lidar waveforms in heterogenous and discrete canopies. IEEE Transactions on Geoscience and Remote Sensing 39 (9), 1943–1958.
Palenichka, R.M., Zaremba, M.B., 2007. Multiscale isotropic matched filtering for individual tree detection in LiDAR images. IEEE Transactions on Geoscience and Remote Sensing 45 (12) (Part 1), 3944–3956.
Reitberger, J., Schnörr, Cl., Krzystek, P., Stilla, U., 2009. 3D segmentation of single trees exploiting full waveform LIDAR data. ISPRS Journal of Photogrammetry and Remote Sensing 64 (6), 561–574.
Sabatini, M.R., Palmerini, G.B., 2008. Differential Global Positioning System (DGPS) for flight testing. NATO Research and Technology Organization, RTO-AG-160 AC/323(SCI-135)TP/189 21, http://ftp.rta.nato.int/public//PubFullText/RTO/AG/RTO-AG-160-V21///$$AG-160-V21-TOC.pdf (Accessed 29 December 2010).
Savage, N., Ndzi, D., Seville, A., Vilar, E., Austin, J., 2003. Radio wave propagation through vegetation: Factors influencing signal attenuation. Radio Science 38 (5), 1088, pp. 1–13, doi:10.1029/2002RS002758.
Seville, A., Craig, K.H., 1995. Semi-empirical model for millimetre-wave vegetation attenuation rates. Electronics Letter 31 (17), 1507–1508.
Smith, D.R., 1993. Digital Transmission Systems, second ed. Van Nostrand Reinhold, New York.
Swanson, A., Huang, S., Crabtree, R., 2009. Using a LiDAR vegetation model to predict UHF SAR attenuation in coniferous forests. Sensors 9 (3), 1559–1573.
Ulaby, F.T., Moore, R.K., Fung, A.K., 1986. Microwave Remote Sensing: Active and Passive Vol III: From Theory to Application. Artech House, Inc..
Ulaby, F.T., Sarabandi, K., McDonald, K., Whitt, M., Dobson, M.C., 1990. Michigan microwave canopy scattering model. International Journal of Remote Sensing 11 (7), 1223–1253.
Violette, E.J., Espeland, R.H., Schwering, F., 1983. Vegetation loss measurements at 9.6, 28.8, and 57.6 GHz through a pecan orchard in Texas. CECOM-83–2, US. Army Communications-Electronics Command, Fort Monmouth, NJ.
Wang, Y., Weinacker, H., Koch, B., 2008. A LiDAR point cloud based procedure for vertical canopy structure analysis and 3D single tree modeling in forest. Sensors 8 (6), 3938–3951.
Weissberger, M.A., 1982. An initial critical summary of models for predicting the attenuation of radio waves by trees. ECAC-TR-81–101. Electromagnetic Compatibility Analysis Center, Annapolis, MD.
Weishampel, J.F., Blair, J.B., Knox, R.G., Dubayah, R., Clark, D.B., 2000. Volumetric lidar return patterns from an old-growth tropical rainforest canopy. International Journal of Remote Sensing 21 (2), 409–415.
Wright, W.C., Liu, P., Slatton, K.C., Shrestha, R.L., Carter, W.E., Lee, H, 2008. Predicting L-band microwave attenuation through forest canopy using directional structure elements and airborne LiDAR. In: Proceedings of IEEE International Geoscience and Remote Sensing Symposium (IGARSS), vol. 3, pp. 688–691.